

Collision cross sections for excitation energy transfer in $\text{Na}^*(3P_{1/2}) + \text{K}(4S_{1/2}) \Leftrightarrow \text{Na}^*(3P_{3/2}) + \text{K}(4S_{1/2})$ processes

V. Horvatic¹, D. Veza¹, M. Movre¹, K. Niemax², C. Vadla¹

¹ Institute of Physics of the University, Bijenicka 46, 10000 Zagreb, Croatia
(Fax: + 385-1/421-156)

² Institut für Physik, Universität Hohenheim, Garbenstrasse 30, D-70599 Stuttgart, Germany
(Fax: + 49-711/459-2461)

Received: 10 February 1995

Abstract. The cross sections for the excitation energy transfer between the 3^2P_J states of sodium atoms by collisions with ground-state potassium atoms have been measured by resonant Doppler-free two-photon spectroscopy, where the population densities of directly pumped and collisionally excited $\text{Na}(3P_J)$ ($J = 1/2, 3/2$) levels were probed by counter-propagating $\text{Na}(3P_J) \rightarrow \text{Na}(4D_{3/2, 5/2})$ excitation and detected with the thermionic diode. Cross sections of $\sigma(3P_{1/2} \rightarrow 3P_{3/2}) = 190 \text{ \AA}^2 \pm 20\%$ and $\sigma(3P_{3/2} \rightarrow 3P_{1/2}) = 100 \text{ \AA}^2 \pm 20\%$ were found. The theoretical calculations taking into account the long-range interaction terms R^{-6} , R^{-8} and R^{-10} yield a value $\sigma(3P_{1/2} \rightarrow 3P_{3/2}) = 165 \text{ \AA}^2$. On the basis of these long-range interaction potentials the differential cross section has been calculated and compared with recently published experimental data. Very good agreement between the theoretical and experimental data was found.

PACS: 34.50; 32.00

1 Introduction

The knowledge of the cross sections for the excitation energy transfer occurring in collision processes involving excited atomic states is important in many fields, both fundamental and applied (see introductions in [1, 2]). The investigations of this phenomenon contribute to basic understanding of atomic structure, interatomic interactions and chemical reactions. The most extensively studied excitation energy transfer processes are those which appear in the collisions involving like or unlike alkali atoms [1, 3]. However, experimental cross sections for one and the same process obtained by different experimental groups are often very different [1]. On the other hand, since alkali atoms have simple hydrogen-like structure the theoretical results should be in reasonable agreement with the experiments. Nevertheless, such agreements

are rare. Considerable improvement of the theoretical results has been achieved lately by calculations emphasizing the role of the long-range interactions of order higher than dipole-dipole one [4].

The present work is an extension, both experimentally and theoretically, of collisional transfer studies in Na^* -dissimilar alkali systems [4] to the case of potassium being collisional partner. The cross sections for the excitation transfer in $\text{Na}^*(3P_{1/2}) + \text{K}(4S_{1/2}) \Leftrightarrow \text{Na}^*(3P_{3/2}) + \text{K}(4S_{1/2})$ processes have been obtained by Doppler-free two-photon technique with thermionic diode detection of population densities in sodium $3P$ levels generated both by collisions and direct optical excitation. It will be shown that very good agreement of the theoretical cross section value with the experimental one is achieved only if the multipole expansion of the long-range potential is not ceased prior to $C_{10} R^{-10}$ term.

To our knowledge, there are only two papers on the Na^* -K system. There is an early experimental paper on the measurement of the total energy transfer cross section [5] (absolute values), and recent one which reports on measurements of the *differential* cross section [6] (relative value). It is expected [1] that the cross sections for fine-structure mixing for various alkali-potassium pairs vary inversely with the fine-structure splitting ΔE_{fs} . From that aspect the cross sections reported in [5] are much too small. For example, they are roughly between 2 to 6 times lower than for the K^* -K system [7–9] and nearly equal to those measured in Rb^* -K case [10]. Additionally, the results in [5] are two times smaller than the well proved cross sections [5, 11, 12] for the same process induced by argon. This is not expected since noble gas-alkali long-range interactions are known to be considerably weaker than those in alkali-alkali systems.

For the mentioned reasons we have reinvestigated the excitation transfer in Na^* -K system by means of laser spectroscopy in order to obtain thermally averaged cross sections. We will compare our present result with the old result [5] as well as with the measurements of the *differential* cross section [6].

2 Experiment

The experimental arrangement is shown in Fig. 1. Distilled potassium metal, containing sodium as a trace element, was placed in the middle of the stainless-steel heat-pipe with Pyrex-glass windows. The metal-vapour mixture was generated in 8 cm long central zone of the heat-pipe, which was resistively heated to temperatures of 485 K – 520 K. For the thermionic diode detection of the collisionally produced ions [13], a molybdenum cathode filament (0.25 mm in diameter) was built in. The measurements were performed in neon buffer gas, its pressure being controlled by MKS Baratron manometer. The metal-vapour pressure ranged from 12 to 45 mTorr in the mentioned temperature range, while the neon pressure was always kept above its value, i.e., between 50 and 100 mTorr, respectively. Neon was chosen as a buffer gas, because among all noble gases it is known to cause the weakest fine-structure mixing in sodium and the smallest line broadening and shift. The metal-vapour mixture was optically excited by two counter-propagating laser beams aligned along the heat-pipe axis. Sodium atoms were excited to one of the fine-structure levels of the first resonance doublet by a modulated (chopper HMS 220) laser beam from a cw single-mode, frequency stabilized ring dye-laser (Spectra Physics, model 380D, dye: RhB) pumped by an argon-ion laser (Spectra Physics model 2030). Since the Na resonance state is far from the ionization limit collisional ionization does not occur. Therefore, there is no thermionic signal from the pump step only. The power of the dye-laser beam was attenuated using neutral density filters and its value after passing through the circular aperture (2 mm in diameter) was typically $15 \mu\text{W}$, i.e., the $\text{Na}(3S_{1/2}) \rightarrow \text{Na}(3P_J)$ ($J = 1/2, 3/2$) transitions were not optically saturated. The optical thickness of the sodium resonance lines was controlled by the measurement of the dye-laser absorption. In the whole temperature range of the investigation the absorption coefficients for $\text{Na}(3S_{1/2}) \rightarrow \text{Na}(3P_J)$ transitions were below 0.1 cm^{-1} , so that there was no radiation trapping [14]. The Na density was determined from the absorption spectra applying the curve of growth method for optically thin lines. The Na atom number density varied in the range from $6 \cdot 10^9 \text{ cm}^{-3}$ to $3 \cdot 10^{10} \text{ cm}^{-3}$. The dispersion of the absorption spectra was calibrated by a confocal Fabry-Perot interferometer with f.s.r. 150 MHz.

The population densities of the $\text{Na}(3P_J)$ levels produced by direct optical excitation or by collisions with potassium atoms were probed by the $\text{Na}(3P_J) \rightarrow \text{Na}(4D_{3/2, 5/2})$ transitions, using a counter-propagating laser beam from a second cw single-mode, frequency stabilized ring-dye laser (Spectra Physics, model 380D, dye: Rh6G) pumped by an argon-ion laser (Spectra Physics model 2020). The thermionic signals, due to collisional ionization of the $4D_J$ sodium atoms, were fed in a lock-in amplifier (Ithaco 391A) operated at reference frequency of 13 Hz. The output was recorded by a three-channel strip-chart recorder (Linseis). The second step dye-laser beam was expanded and its power attenuated by neutral density filters. The beam in the heat-pipe had a diameter of 8 mm. The power used for checking collisionally populated sodium levels varied in the range between 1 and 10 mW depending on

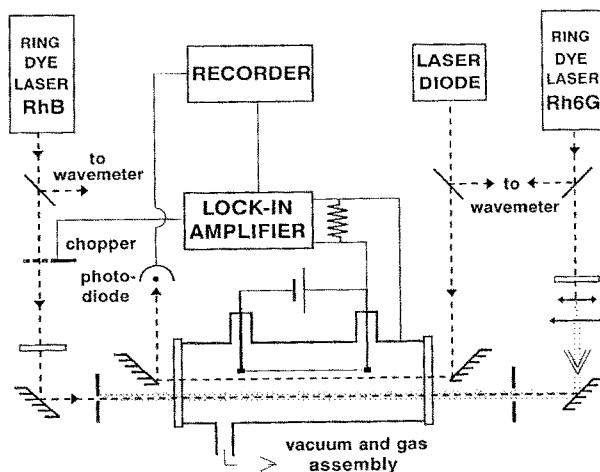


Fig. 1. Experimental arrangement

the particular temperature, i.e., atom number density of the potassium atoms inducing the excitation transfer. For probing the population density generated by direct excitation of Na atoms the power used was in the range 10–100 μW . Although the oscillator strengths of the $\text{Na}(3P_J) \rightarrow \text{Na}(4D_{3/2, 5/2})$ transitions are small (according to [15] almost one order of magnitude lower than for $\text{Na}(3S_{1/2}) \rightarrow \text{Na}(3P_J)$ transitions) the measured thermionic signals were checked for possible optical saturation. It was assured that none occurred even at the highest power used. The dispersion of the $\text{Na}(3P_J) \rightarrow \text{Na}(4D_{3/2, 5/2})$ spectra was marked by transmission peaks of another 150 MHz f.s.r. Fabry-Perot interferometer.

The potassium atom number density was determined from the absorption coefficient in the wing of the potassium D1 line. The appropriate laser radiation was supplied by a single-mode, frequency stabilized laser diode (Sharp LTO27MDO, $\lambda = 777 \text{ nm}$ at $T = 25^\circ\text{C}$, power: 7 mW). The absorption spectrum was calibrated by a 2 GHz f.s.r. confocal Fabry-Perot interferometer. The diode laser beam had a diameter of 2 mm and power was reduced to $15 \mu\text{W}$ by optical filters. The potassium atom number density changed from $2.9 \cdot 10^{14} \text{ cm}^{-3}$ to $1 \cdot 10^{15} \text{ cm}^{-3}$ in the experimental temperature range.

3 Data analysis and results

Figure 2 shows the partial term diagram of the sodium atom comprising the radiative and collisional rates relevant in a simple three-level model used. Since the cross section values for the interalkali excitation transfer are at least one order of magnitude lower than the ones for the intramultiplet mixing [1, 3], the rate corresponding to the excitation transfer from Na to K has been disregarded in the rate equations.

If the sodium $3P_{1/2}$ state is excited by laser radiation the steady-state equation for the population density of collisionally populated $\text{Na}(3P_{3/2})$ level is given by:

$$\frac{d}{dt} N^{\text{sens}}(3P_{3/2}) = 0 = CN^{\text{dir}}(3P_{1/2}) - (A^* + D) N^{\text{sens}}(3P_{3/2}), \quad (1)$$

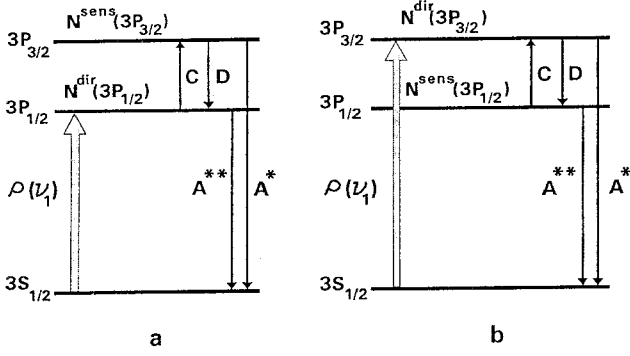


Fig. 2a, b. Partial sodium term diagram with the collisional and radiative rates when the $3P_{1/2}$ state a, or the $3P_{3/2}$ state b are optically excited. The details regarding the rates shown are given in Sect. 3

where $N^{\text{dir}}(3P_{1/2})$ and $N^{\text{sens}}(3P_{3/2})$ label the population densities of the optically pumped $\text{Na}(3P_{1/2})$ and collisionally excited $\text{Na}(3P_{3/2})$ level, respectively (notation was chosen in analogy with direct and sensitized fluorescence), A^* denotes the spontaneous emission coefficient of the $\text{Na}(3P_{3/2})$, while C and D are the fine-structure collisional mixing rates. The steady-state population density of the $\text{Na}(3P_{1/2})$ level, while $\text{Na}(3P_{3/2})$ being optically excited, is described by:

$$\frac{d}{dt} N^{\text{sens}}(3P_{1/2}) = 0 = DN^{\text{dir}}(3P_{3/2}) - (A^{**} + C) N^{\text{sens}}(3P_{1/2}), \quad (2)$$

where A^{**} is the spontaneous emission coefficient for $\text{Na}(3P_{1/2}) \rightarrow \text{Na}(3S_{1/2})$ transition. For optically thin conditions and the absence of the radiation trapping, the spontaneous emission coefficients are equal, i.e., $A^{**} = A^* = A$, thus the solution of the set of the (1) and (2) exhibits the form:

$$C = A \frac{\eta_C + \eta_C \eta_D}{1 - \eta_C \eta_D}, \quad (3)$$

$$D = A \frac{\eta_D + \eta_C \eta_D}{1 - \eta_C \eta_D}, \quad (4)$$

where

$$\eta_C = \frac{N^{\text{sens}}(3P_{3/2})}{N^{\text{dir}}(3P_{1/2})}, \quad (5)$$

$$\eta_D = \frac{N^{\text{sens}}(3P_{1/2})}{N^{\text{dir}}(3P_{3/2})}. \quad (6)$$

The numerical results have been evaluated using the value $A = 6.2 \cdot 10^7 \text{ s}^{-1}$ [15].

In analogy with gas kinetics, fine-structure collisional transfer rates C and D are of the form $\sigma \bar{v} N$, where \bar{v} is the mean relative velocity of the colliding atoms, N is the number density of the atoms inducing the excitation transfer and σ is the corresponding effective cross section.

Since the heat-pipe was not operated in heat-pipe mode, the experimentally determined values for the rates C and D include the contributions due to collisions with potassium and neon atoms. Assuming the validity of the binary approximation, the measured rates can be expressed in the following way:

$$C = \sigma_C^{\text{Na-K}} \bar{v}_{\text{Na-K}} N_{\text{K}} + \sigma_C^{\text{Na-Ne}} \bar{v}_{\text{Na-Ne}} N_{\text{Ne}}, \quad (7)$$

$$D = \sigma_D^{\text{Na-K}} \bar{v}_{\text{Na-K}} N_{\text{K}} + \sigma_D^{\text{Na-Ne}} \bar{v}_{\text{Na-Ne}} N_{\text{Ne}}. \quad (8)$$

Here σ_C and σ_D denote the cross sections for the $\text{Na}(3P_{1/2}) \rightarrow \text{Na}(3P_{3/2})$ and $\text{Na}(3P_{3/2}) \rightarrow \text{Na}(3P_{1/2})$ processes, respectively, while N_{K} and N_{Ne} are the ground-state atom number densities of the potassium and neon, respectively.

Contributions due to collisions between the excited and ground-state sodium atoms have been neglected since the sodium number density is small. Taking into account the cross sections for sodium fine-structure mixing induced in Na^*-Na collisions [16] and the experimental sodium atom number densities, this rate is a few orders of magnitude lower than the rate due to Na^*-K collisions only.

Applying the Dalton's law to the total pressure in the central heat-pipe zone, and expressing the partial pressures by the ideal-gas equation, the neon atom number density in the metal-vapour column was calculated using the value for the total pressure measured with manometer and experimentally determined values for N_{K} and temperature. In the evaluation of the data we used the cross sections $\sigma_C^{\text{Na-Ne}} = 67 \text{ \AA}^2$ and $\sigma_D^{\text{Na-Ne}} = 35 \text{ \AA}^2$ given by [11].

The temperature of the metal vapour was determined by fit of the sodium D1 and D2 absorption lines to Doppler profiles, leaving the temperature as a free parameter. By this procedure the temperature could be determined with an uncertainty of $\pm 15 \text{ K}$ which, in the working temperature range, yields a statistical accuracy of $\pm 3\%$. The temperature was necessary for the determination of the mean relative velocities of the colliding species ($\bar{v}_{\text{Na-K}}, \bar{v}_{\text{Na-Ne}}$) and the neon atom number density N_{Ne} using the ideal-gas equation. Due to the error in the vapour temperature determination, the error of the relative velocities was about $\pm 1.5\%$.

The potassium ground-state atom number density was determined from the measurement of the absorption coefficient $k(\Delta\nu)$ in the resonance wing of the potassium D1 line. The actual length of the absorbing column was estimated to $L = (5 \pm 0.5) \text{ cm}$. The absorption coefficient was determined from the impact region of the line wing ($8 \text{ GHz} < \Delta\nu < 14 \text{ GHz}$), where $k(\Delta\nu)$ exhibits the usual Lorentzian form:

$$k(\Delta\nu) = \frac{\pi e^2}{mc} f N_{\text{K}} \frac{\Gamma}{2\pi(\Delta\nu)^2}. \quad (9)$$

In (9) Γ is the half-width (FWHM) of the Lorentzian profile and f is the oscillator strength of the potassium D1 line. The half-width is given by:

$$\begin{aligned} \Gamma &= \Gamma_N + \Gamma_{\text{K-Ne}} + \Gamma_{\text{K-K}} \\ &= \Gamma_N + \gamma_{\text{K-Ne}} N_{\text{Ne}} + \gamma_{\text{K-K}} N_{\text{K}}, \end{aligned} \quad (10)$$

where Γ_N is the natural half-width, Γ_{K-Ne} and Γ_{K-K} are the half-widths due to the K-Ne and K-K broadening, respectively, which can be expressed in the product form of the reduced half-widths γ for the particular broadening and the corresponding number density of atoms causing the broadening. The numerical values of the quantities in (10) are as follows: $\Gamma_N = 6.05$ MHz [9], $\gamma_{K-Ne} = 2.71 \cdot 10^{-10} \text{ s}^{-1} \text{ cm}^3$ (experimentally obtained by [17] with accuracy of about 2%), $\gamma_{K-K} = 1.03 \cdot 10^{-7} \text{ s}^{-1} \text{ cm}^3$ (theoretical value in the impact region given by [18, 19]). Subsequent to all necessary substitutions (9) yields the quadratic equation for N_K :

$$k(\Delta\nu) = \frac{9.03 \cdot 10^{-11}}{(\Delta\nu)^2} N_K^2 + \frac{1.43 \cdot 10^{-3}}{(\Delta\nu)^2} \times (\Gamma_N + 2.71 \cdot 10^{-10} \cdot \alpha) N_K. \quad (11)$$

Here, $\alpha = p/k_B T$, where p is the total gas pressure, k_B is the Boltzmann constant and T is the temperature in the central zone of the heat-pipe. In (11) $\Delta\nu$ is measured in s^{-1} , N_K , α are in cm^{-3} , and $k(\Delta\nu)$ in cm^{-1} .

Taking into account the highest buffer gas pressure used in the measurements (0.1 Torr) and the uncertainty in the temperature determination, one finds that the accuracy of α is about $\pm 3\%$. This affects the coefficient of the linear term in (11) by less than 1%, which consequently results with a negligible uncertainty in the determination of N_K . In order to check for possible systematic error introduced by the choice of values for noble-gas broadening constants, we have determined N_K also in another way. Subsequent to the standard absorption measurement, we have measured the absorption in double path through the heat-pipe in order to arise the quasistatic part of the resonance wing. From the measurements of the absorption coefficient along the red quasistatic wing of K D1 line it was possible to determine N_K applying the method described in [20] which yields reliable results for

the atom number density and does not require knowledge about the vapour temperature. The difference between the values for N_K determined in both ways was less than 10%.

Typical spectra for the measurement of the population ratios η_C and η_D are shown in Fig. 3. Additionally, the corresponding excitation diagrams are given. The pump laser was locked to the centre of the $\text{Na}(3S_{1/2}) \rightarrow \text{Na}(3P_{1/2})$ (Fig. 3a) or $\text{Na}(3S_{1/2}) \rightarrow \text{Na}(3P_{3/2})$ transition (Fig. 3b). Note that in this case Na atoms with the velocity component $v_z \approx 0$ with respect to the direction of the laser beam are excited. Therefore, as shown in [21], the mean relative velocity of this particular velocity group is Maxwellian. The frequency of the probe laser was tuned across the $\text{Na}(3P_{1/2,3/2}) \rightarrow \text{Na}(4D_{3/2,5/2})$ line. The thermionic signals of the directly pumped $3P_{1/2}$ and collisionally sensitized $3P_{3/2}$ levels are denoted as $S_{1/2}^{\text{dir}}$ and $S_{3/2}^{\text{sens}}$, respectively. The analogous signals obtained by the optically excited $\text{Na}(3P_{3/2})$ and collisionally induced $\text{Na}(3P_{1/2})$ populations, are labelled with $S_{3/2}^{\text{dir}}$ and $S_{1/2}^{\text{sens}}$, respectively. The spectra which are obtained from the directly excited $\text{Na}(3P_j)$ levels are Doppler-free. They display the hyperfine structure of the Na ground-state level. The transfer spectra exhibit much broader shapes due to the velocity changes in the collision transfer process. However, the $\text{Na}(3S_{1/2})$ hyperfine splitting and the partially resolved hyperfine structure of $\text{Na}(3P_j)$ levels can also be seen.

The presented spectra were obtained at temperature $T = 515$ K and Ne pressure of 80 mTorr. The potassium and sodium densities were $N_K = 7.1 \cdot 10^{14} \text{ cm}^{-3}$ and $N_{Na} = 2.2 \cdot 10^{10} \text{ cm}^{-3}$, respectively, while the partial pressure of neon in the metal vapour zone corresponded to $N_{Ne} = 7.8 \cdot 10^{14} \text{ cm}^{-3}$.

With all relevant parameters being kept fixed, the integral thermionic signals $S = \int S(\nu) d\nu$ is proportional to the product of the laser power density $\rho(\nu_2)$, the population density of the $\text{Na}(3P_j)$ level in question and Einstein absorption coefficient $B(3P \rightarrow 4D)$. Therefore, according

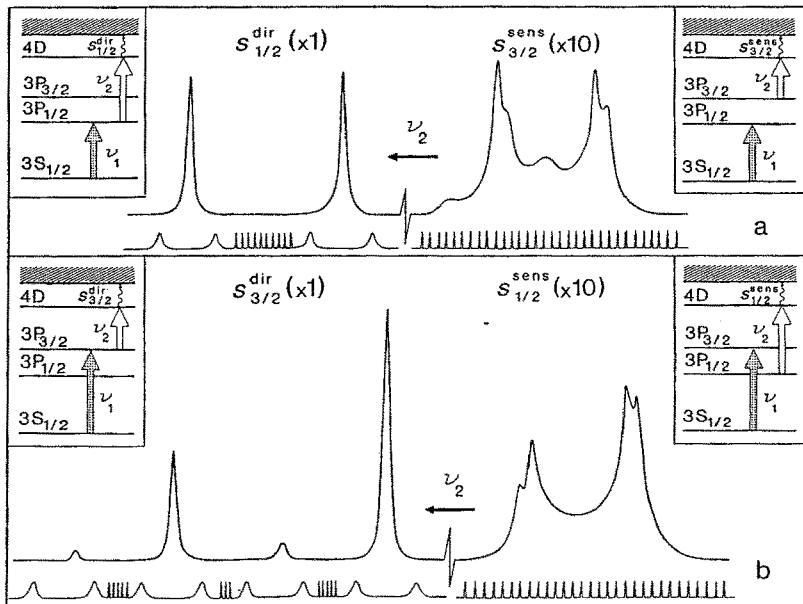


Fig. 3a, b. Spectra measured with the thermionic diode. a Shows the spectra $S_{1/2}^{\text{dir}}$ and $S_{3/2}^{\text{sens}}$ obtained by scanning the second step laser over the $\text{Na}(3P_{1/2}) \rightarrow \text{Na}(4D_{3/2})$ and $\text{Na}(3P_{3/2}) \rightarrow \text{Na}(4D_{3/2,5/2})$ transitions, respectively, while the $\text{Na } 3P_{1/2}$ level is directly optically excited. b Shows the analogous spectra for $\text{Na } 3P_{3/2}$ level pumping. The hyperfine splitting of the $\text{Na } 3S_{1/2}$ and $\text{Na } 3P_{1/2}$ level, as well as partly resolved hyperfine structure of $\text{Na } 3P_{3/2}$ state can be observed. The dispersion calibration marks are separated by 150 MHz

to (5) and (6) η_C and η_D can be expressed by:

$$\eta_C = \frac{S_{3/2}^{\text{sens}} \rho_{\text{dir}}(v_2) B(3P_{1/2} \rightarrow 4D_{3/2})}{S_{1/2}^{\text{dir}} \rho_{\text{sens}}(v_2) B(3P_{3/2} \rightarrow 4D_{3/2, 5/2})}, \quad (12)$$

$$\eta_D = \frac{S_{1/2}^{\text{sens}} \rho_{\text{dir}}(v_2) B(3P_{3/2} \rightarrow 4D_{3/2, 5/2})}{S_{3/2}^{\text{dir}} \rho_{\text{sens}}(v_2) B(3P_{1/2} \rightarrow 4D_{3/2})}. \quad (13)$$

Taking into account the oscillator strengths for the $3P \rightarrow 4D$ transitions given in [15], the B coefficients in the above equations are equal.

With the pairs of experimentally determined η_C and η_D values, the total collisional rates C and D have been evaluated according to (3) and (4), respectively. The collisional rates for the particular process of interest, i.e., $C_{\text{Na-K}} = \sigma_C^{\text{Na-K}} \bar{v}_{\text{Na-K}} N_K$ and $D_{\text{Na-K}} = \sigma_D^{\text{Na-K}} \bar{v}_{\text{Na-K}} N_K$, were calculated using (7) and (8). In Fig. 4 $C_{\text{Na-K}}$ and $D_{\text{Na-K}}$ divided by the corresponding mean relative velocity $\bar{v}_{\text{Na-K}}$ are plotted against the potassium atom number density. The straight lines represent least square fits through the experimental points. Within the experimental error bar, these straight lines intercept the ordinate at the origin. The slopes of the straight lines yield the following cross-sections:

$$\sigma_C^{\text{Na-K}} = 190 \text{ \AA}^2$$

for the $\text{Na}^*(3P_{1/2}) + \text{K}(4S_{1/2}) \rightarrow \text{Na}^*(3P_{3/2}) + \text{K}(4S_{1/2})$ process, and

$$\sigma_D^{\text{Na-K}} = 100 \text{ \AA}^2$$

for the $\text{Na}^*(3P_{3/2}) + \text{K}(4S_{1/2}) \rightarrow \text{Na}^*(3P_{1/2}) + \text{K}(4S_{1/2})$ process.

The experimental cross sections have a ratio of 1.9. The principle of detailed balancing, for our experimental conditions ($T = 502 \text{ K}$) yields $\sigma_C/\sigma_D = 2\exp(-24.5/T) = 1.90$.

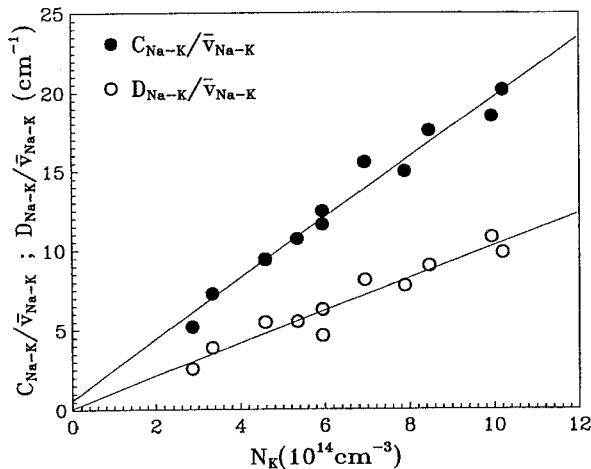


Fig. 4. The measured rates for the sodium $3P$ fine-structure excitation transfer by potassium, divided by the relative velocity of collision partners in dependence on the potassium atom number density. The rates $C_{\text{Na-K}}$ and $D_{\text{Na-K}}$ are representing $3P_{1/2} \rightarrow 3P_{3/2}$ and $3P_{3/2} \rightarrow 3P_{1/2}$ transfer processes, respectively. The straight lines are the least square fits through the experimental data

We estimate an overall experimental uncertainty of the cross sections to be $\pm 20\%$. The error includes inaccuracy of the temperature and the potassium number density, as well as the statistical error of the least square fits.

4 Theoretical calculation

The theoretical calculations of the cross section for sodium $3P$ fine-structure excitation transfer induced by collisions with potassium ground-state atoms have been performed in the same way already employed for $\text{Na}^*\text{-Rb}$ and $\text{Na}^*\text{-Cs}$ systems [4]. In the following the procedure is briefly outlined.

An alkali atom A in the first excited P state is being perturbed by alkali atom B in the ground-state. If one neglects the fine structure in the perturber states, the long-range pattern for the system $A^*(P_J) + B(S_{1/2})$ is simple [22, 23]. It consists of three groups of the potentials, one with $\Omega = 0^+, 0^-, 1$, stemming from the $P_{1/2}$ asymptote, and the other two with $\Omega = 0^+, 0^-, 1$ and $\Omega = 1, 2$ stemming from the $P_{3/2}$ asymptote. The Hamiltonian matrix in diabatic basis of atomic product states for pairs $0^+, 0^-$ or 1 potentials (the other $1, 2$ states remain uncoupled) exhibits the form:

$$H_{11} = U_0 - \frac{\Delta\varepsilon + V}{2}, \quad (14)$$

$$H_{22} = U_0 + \frac{\Delta\varepsilon + V}{2}, \quad (15)$$

$$H_{12} = H_{21} = \sqrt{2}V. \quad (16)$$

Here the labels 1 and 2 refer to the $P_{1/2}$ and $P_{3/2}$ states, respectively, $\Delta\varepsilon$ is the fine-structure splitting of the P_J level in question, while U_0 and V are defined by:

$$U_0 = \frac{\Delta\varepsilon}{2} + \frac{V^\Sigma + V^\Pi}{2}, \quad (17)$$

$$V = \frac{V^\Sigma - V^\Pi}{3}. \quad (18)$$

The V^Σ and V^Π are the adiabatic potentials obtained with + neglecting the fine-structure of the P level. The multipole expansion

$$V = C_6 R^{-6} + C_8 R^{-8} + \dots, \quad (19)$$

applies well to the potentials in the long-range region. Above, R is the internuclear distance and C_n constants are according to (18) given by:

$$C_n = \frac{C_n^\Sigma - C_n^\Pi}{3}. \quad (20)$$

The coupled equations for the probability amplitudes $c_1(t)$ and $c_2(t)$ for the two states labelled with 1 and 2, obtained within a simplified semiclassical treatment of a two-state

collision problem [24] are as follows:

$$i\hbar \frac{d}{dt} c_1 = H_{11}c_1 + H_{12}c_2, \quad (21)$$

$$i\hbar \frac{d}{dt} c_2 = H_{21}c_1 + H_{22}c_2. \quad (22)$$

The initial conditions are $|c_1(t = -\infty)| = 1$ and $c_2(t = -\infty) = 0$. The time dependence of the matrix elements H_{ij} is introduced assuming a straight-line trajectory $R(t) = \sqrt{b^2 + \bar{V}^2 t^2}$, where b is the impact parameter and \bar{V} is the mean relative velocity of the colliding atoms. The cross section σ is determined according to

$$\sigma = 2\pi \int_0^{\infty} P(b) b db \quad (23)$$

where $P(b) = |c_2(t = +\infty)|^2$. Since the U_0 part of H_{ij} leads to the common phase of c_i , for the problem being considered the set of (21) and (22) is fully equivalent to:

$$i\hbar \frac{d}{dt} a_1 = \frac{\Delta\varepsilon + V}{2} a_1 + \sqrt{2} V a_2, \quad (24)$$

$$i\hbar \frac{d}{dt} a_2 = \sqrt{2} V a_1 + \frac{\Delta\varepsilon + V}{2} a_2, \quad (25)$$

where $|a_i(t)|^2 = |c_i(t)|^2$.

The numerical calculations of the cross sections have been carried out for two sets of the values for C_n constants for Na($3P_{1/2}$) + K($4S_{1/2}$) system, obtained by different authors. The first one is that given by [25], which after being transformed in accordance with the definition (20) of C_n constants, results with: $C_6 = 3.67 \cdot 10^{-31} \text{ cm}^6 \text{ s}^{-1}$, $C_8 = -3.30 \cdot 10^{-45} \text{ cm}^8 \text{ s}^{-1}$. The C_n constants of higher order have not been given in [25]. The second set of C_n values has been calculated by [26] and their values are: $C_6 = 3.18 \cdot 10^{-3} \text{ cm}^6 \text{ s}^{-1}$, $C_8 = -3.17 \cdot 10^{-45} \text{ cm}^8 \text{ s}^{-1}$, $C_{10} = -1.48 \cdot 10^{-59} \text{ cm}^{10} \text{ s}^{-1}$.

As already discussed in [4], in first approximation, taking the dipole-dipole term $C_6 R^{-6}$ only, the calculation yields substantially lower cross section than observed. The region of impact parameters $b > 6 \text{ \AA}$ contributes to the cross section with only 6 \AA^2 . For lower values of b , where transition probability $P(b)$ begins to oscillate with maximal amplitude, the assumed form of the potential is not applicable at all. From (24) and (25) it is clear that, besides fine-structure splitting $\Delta\varepsilon$, which is fixed in our case, the only variable parameter of the model is the function V defined by (18). Taking only the leading term of (19), the function V monotonically grows with decreasing R , but inclusion of higher terms introduces a maximum, causing the function $P(b)$ to begin to be significant for impact parameters below 10 \AA (see Fig. 5b in the next section).

Taking into account the $C_8 R^{-8}$ term we have obtained $\sigma_C^{\text{Na-K}} = 140 \text{ \AA}^2$ and $\sigma_D^{\text{Na-K}} = 145 \text{ \AA}^2$, using the first and the second set of C_n constants, respectively. As it has been already found for the Na*-Rb and Na*-Cs systems [4], the inclusion of the dipole-quadrupole interaction substantially influences the result. Our final value, obtained by taking into account the long-range interaction terms up to R^{-10} is $\sigma_C^{\text{Na-K}} = 165 \text{ \AA}^2$. This datum is within the error bar of our experimental value. In the

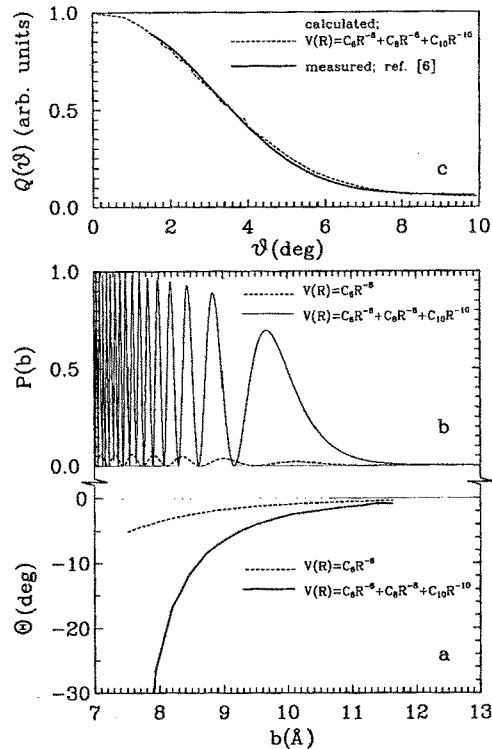


Fig. 5. a Part displays the deflection angle as a function of impact parameter obtained if scattering by solely dipole-dipole interaction is assumed (*broken curve*) and in the case when higher order interaction terms are taken into account (*full curve*). In the b part of the figure the transition probability for the process Na($3P_{1/2}$) + K($4S_{1/2}$) \rightarrow Na($3P_{3/2}$) + K($4S_{1/2}$) as a function of impact parameter is displayed. *Broken curve*: the result obtained with only dipole-dipole interaction taken into account; *full curve*: the result obtained with terms up to R^{-10} being included. c Displays differential cross section for Na fine-structure transfer induced by K collisions as a function of scattering angle; *Broken curve*: experimental result obtained by [6]; *full curve*: calculated assuming the scattering by the long-range potential of the form $C_6 R^{-6} + C_8 R^{-8} + C_{10} R^{-10}$.

calculations we have used mean relative velocity $\bar{V} = 8.6 \cdot 10^4 \text{ cm s}^{-1}$, which corresponds to the average temperature in our experiment (502 K).

5 Discussion

The only paper on the total cross sections for the excitation transfer process Na*($3P_{1/2}$) + K($4S_{1/2}$) \leftrightarrow Na*($3P_{3/2}$) + K($4S_{1/2}$) published by Seiwert almost forty years ago [5] reports the following cross sections for temperatures in the range 540 K to 564 K: $\sigma_C^{\text{Na-K}} = 65 \text{ \AA}^2$ and $\sigma_D^{\text{Na-K}} = 45 \text{ \AA}^2$. Note that the experimental cross section ratio $\sigma_C^{\text{Na-K}}/\sigma_D^{\text{Na-K}} = 1.44$ is in considerable disagreement with the prediction of detailed balancing, which yields 1.91 at $T = 552 \text{ K}$. In the paper [5] the cross sections were obtained at high optical depth of sodium D lines and the excitation radiation was supplied by a resonance lamp. Detailed calculations regarding the source intensity, spectral profile and escaping fluorescence intensity dependence on depth into the vapour were necessary

for evaluation of the results. Nevertheless, the effective spontaneous emission rates of sodium D lines which were used are in fair agreement with more recent values obtained by time-resolved measurements of the fluorescence decay rates following pulsed excitation [16]. The major objection on the measurements lies in the fact that neither the Na nor the K atom number density were measured. Both these data were required for determination of the cross section since contribution by Na^*-Na collision could not be neglected. In paper [5] the number densities were calculated applying Raoult's law for partial pressures of the elements for ideal binary mixture using the vapour pressure curves of the pure elements at the experimental temperature. Atom number densities obtained in this way can be very inaccurate, first because the vapour pressure curves themselves are not known very accurately, and second they are subject to an uncertainty introduced by the dependence of the partial pressure for the particular component on its mole fraction. In [5] it was only stated that it was 50% mole solution but the possible error bar for this quantity was not given. Also it has to be noted that the Seiwert's cross sections for the sodium fine-structure mixing induced by potassium are two times smaller than the well proved cross sections [5, 11, 12] for the same process induced by argon. This is surprising since noble gas-alkali long range interactions are known to be considerably weaker than those in alkali-alkali systems.

As mentioned above, there is a recent work on the Na^*-K collisional system [6] where the *differential* cross section for the $\text{Na}^*(3P_{3/2}) + \text{K}(4S_{1/2}) \rightarrow \text{Na}^*(3P_{1/2}) + \text{K}(4S_{1/2})$ process has been measured in a crossed alkali beams experiment. In this paper was found that only $\sim 25\%$ of the observed cross section (when weighted by solid angle $d\Omega$) is at scattering angles $\vartheta < 5^\circ$. The authors stated that this portion corresponds to the atoms scattered by the C_6R^{-6} interaction at impact parameters greater than about 8 \AA . In order to get more insight in the physics involved, we have investigated the scattering process in the classical approximation [24].

Classical mechanics offers a simple description of atomic collision processes which has proven to give a valuable qualitative understanding of the full quantal problem [27]. First, one has to calculate a deflection function $\theta(b)$. For typical interatomic potential describing the long-range attraction and short-range repulsion, the deflection angle θ acquires different signs depending on impact parameter b . The scattering angle ϑ observed in the experiment, which by definition varies over the range $0 \leq \vartheta \leq \pi$, equals $\vartheta = \min |\theta - 2\pi n|$, $n = 0, \pm 1, \pm 2, \dots$, where n counts the number of circulations around the centre. The inverse function $b(\vartheta)$ is, generally speaking, multivalued. A *differential* cross section $Q(\vartheta)$ for an inelastic scattering process is then given by:

$$Q(\vartheta) = \sum_i P(\vartheta) \frac{b_i}{\sin \vartheta} \left| \frac{db}{d\vartheta} \right|_i. \quad (26)$$

Here the subscript i distinguishes the various values of b which contribute to the same value of ϑ . The $P_i(\vartheta)$ can be interpreted as the transition probability in classical

scattering (quantity $P(b)$ displayed in Fig. 5b) specified by the deflection angle $\theta(b_i)$ for trajectory with impact parameter b_i .

For collision energies lower than a critical value E_c the deflection function θ has a logarithmic singularity at the orbiting impact parameter b_0 and there is an infinite number of impact parameters b_i contributing to the scattering angle ϑ . However, for scattering through small angles, $\vartheta \ll 1$, the main contribution is given by outermost b_i , which probes the long-range part of the interatomic potential.

Figure 5a shows the deflection angle θ calculated for the potential $V(R) = C_6R^{-6} + C_8R^{-8} + C_{10}R^{-10}$ with C_n from [26] (solid line). The orbiting singularity occurs at $b_0 = 7.5 \text{ \AA}$. The dashed line represents the deflection function which is obtained if the potential assumes the truncated form C_6R^{-6} . In this case there is also an orbiting singularity below 7 \AA , but still in the region of impact parameters where the corresponding transition probability (see Fig. 5b) is very low implying that the resulting differential cross section would be one order of magnitude smaller than in the former case. For impact parameters $b \gtrsim 9 \text{ \AA}$, which correspond to $\vartheta \leq 5^\circ$, the high-energy approximation $V/E \ll 1$ is valid, and for the additive potential V the deflection angle is additive too. This indicates that even in the region of the small ϑ the dipole-quadrupole contribution accounts for the major part of the scattering angle and is capable to scatter particles much more effectively than dipole-dipole contribution alone.

Finally, Fig. 5c shows the *differential* cross section $Q(\vartheta)$ which was appropriately broadened in order to enable comparison with the experimental findings [6]. It was calculated according to (26) in which we have used the results for $P(b)$ and $\theta(b)$ displayed in Fig. 5a and b, respectively. The good agreement between the measured and calculated differential cross sections could be partly fortuitous, bearing in mind the experimental resolution of $\sim 2^\circ$ which smears out all oscillations caused either by $P(\vartheta)$ or, in particular for higher angles, by quantum interferences of various trajectories contributions.

The above analysis brings us to the conclusion that the dipole-quadrupole interaction not only accounts for the major part of the measured effective cross section reported here, but is also responsible for the part of the *differential* cross section which appears at the scattering angles $\vartheta > 5^\circ$, and which at the same time constitutes the major fraction (75%) of the observed *differential* cross section [6].

6 Conclusion

We have reinvestigated the process of excitation energy transfer between fine-structure levels of the sodium first resonance state induced by collisions with the ground-state potassium atoms, applying resonant Doppler-free two-photon laser spectroscopy with thermionic diode detection. We obtained values 190 \AA^2 and 100 \AA^2 for $\text{Na}(3P_{1/2}) \rightarrow \text{Na}(3P_{3/2})$ and $\text{Na}(3P_{3/2}) \rightarrow \text{Na}(3P_{1/2})$ transfer, respectively. Their ratio of 1.9 coincides with the prediction of the detailed balancing which is 1.90 at the

average temperature in our experiment (502 K). The theoretical calculations on the basis of the long-range interaction potentials for Na–K pair yield the cross section of 165 \AA^2 for $\text{Na}(3P_{1/2}) \rightarrow \text{Na}(3P_{3/2})$ transfer. The latter value, which is within the error bar of our experimental result, was obtained with the inclusion of the $C_{10} R^{-10}$ term in multipole expansion of the interaction potential. If only dipole-dipole interaction is involved the theoretical value is considerably lower than the experimental datum. Therefore, we conclude that the investigated mixing process is caused by long-range potential and dominated by the terms in the multipole expansion higher than the dipole-dipole interaction. The importance of these terms was already demonstrated for the broadening of the sodium *D* lines by K, Rb and Cs [22] and for the Na fine-structure transfer induced by Rb and Cs collisions [4]. Additionally, a simple classical calculation of the *differential* cross section and the comparison with previously reported measurements [6] show that the dipole-quadrupole interaction is responsible for the contribution observed at scattering angles larger than 5° which at the same time constitutes the major fraction of the measured *differential* cross section.

The agreement between the measured and calculated values for the cross section can be regarded good. This is encouraging regarding, up to recently [4], almost proverbial differences between experiment and theory in this area [1].

The authors wish to thank the Deutsche Forschungsgemeinschaft (project No. Ni 185/17) and Ministry of Science of the Republic of Croatia, for financial support.

References

1. Krause, L.: In: *The excited state in chemical physics*. McGowan, J.W. (ed.), p. 267. New York: Wiley 1975
2. Brust, J., Veza, D., Movre, M., Niemax, K.: *Z. Phys.* **D32**, 305 (1995)
3. Lewis, E. L.: *Phys. Rep.* **58**, 1 (1980)
4. Vadla, C., Movre, M., Horvatic, V.: *J. Phys.* **B27**, 4611 (1994)
5. Seiwert, R.: *Ann. Phys.* **18**, 54 (1956)
6. Arcuni, P. W., Troyer, M. L., Gallagher, A.: *Phys. Rev.* **A41**, 2398 (1990)
7. Hoffman, K., Siewert, R.: *Ann. Phys.* **7**, 71 (1961)
8. Chapman, G.D., Krause, L.: *Can. J. Phys.* **44**, 753 (1966)
9. Thangaraj, M.A.: Ph.D. Thesis, University of Toronto 1948
10. Vadla, C., Knezovic, S., Movre, M.: *J. Phys.* **B25**, 1337 (1992)
11. Pitre, J., Krause, L.: *Can. J. Phys.* **45**, 2671 (1967)
12. Jordan, J. A., Franken, P. A.: *Phys. Rev.* **142**, 20 (1966)
13. Niemax, K.: *Appl. Phys.* **B38**, 147 (1985)
14. Holstein, T.: *Phys. Rev.* **72**, 1212 (1947)
15. Hansen, W.: *J. Phys.* **B17**, 4833 (1984)
16. Huennekens, J., Gallagher, A.: *Phys. Rev.* **A27**, 1851 (1983)
17. Lwin, N., McCartan, D. G.: *J. Phys.* **B11**, 3841 (1978)
18. Stacey, D. N., Cooper, J.: *Phys. Lett.* **30A**, 49 (1969)
19. Carrington, C. G., Stacey, D. N., Cooper, J.: *J. Phys.* **B6**, 417 (1973)
20. Horvatic, V., Movre, M., Beuc, R., Vadla, C.: *J. Phys.* **B26**, 3679 (1993)
21. Vadla, C., Lawrenz, J., Niemax, K.: *Opt. Comm.* **63**, 63 (1987)
22. Vadla, C., Niemax, K.: *Z. Phys.* **A315**, 263 (1984)
23. Movre, M., Beuc, R.: *Phys. Rev.* **A31**, 2957 (1985)
24. Child, M. S.: *Molecular collision theory*. New York: Academic Press 1974
25. Bussery, B., Achkar, Y., Aubert-Frécon, M.: *Chem. Phys.* **116**, 319 (1987)
26. Spelsberg, D., Meyer, W.: Private communication
27. Korsch, H. J., Thylwe, K. E.: *J. Phys.* **B16**, 793 (1983)